Research Journal of Applied Sciences, Engineering and Technology 12(5): 607-611, 2016
DOI:10.19026/rjaset.12.2689
ISSN: 2040-7459; e-ISSN: 2040-7467

Submitted: October 9, 2015 Accepted: October 30, 2015 Published: March 05, 2016

Research Article

Quantum Efficiency Effects on Modal Gain, Threshold Current and Threshold Current Density of PbSe/$Pb_{0.934}Sr_{0.066}$ Se Multiple Quantum Well Structure

Majed Khodr
Department of Electronics and Communications Engineering, American University of Ras Al Khaimah, P.O. Box 10021, Ras Al Khaimah, United Arab Emirates

Abstract: In this study we studied the effects of internal quantum efficiency on PbSe/$Pb_{0.934}Sr_{0.066}$ Se multiple Quantum well Structure. The calculations were done on the modal gain, threshold current and threshold current density of the system. Inclusion of the theoretical internal quantum efficiency increased the threshold current and threshold current density values by almost 10 times with no effects on the modal gain values. However, when the experimental internal quantum efficiency was included, the above increase was even more. It was included that there is a leakage current above the barrier which is needed to account for in any practical application.

Keywords: Auger recombination, leakage current, lead salts, quantum efficiency

INTRODUCTION

An attractive aspect of IV-VI lead salts semiconductor materials is that they can be grown with high crystalline quality on industry standard silicon substrates (Lehtinen and Kuusela, 2014; Razeghi *et al*., 2013; Yang *et al*., 2005; Kim *et al*., 2007). Such a growth technology can be readily scaled to enable low unit cost production thus making possible the commercialization of low cost sensors for the widest possible distribution. This study focuses on the physics and engineering of IV-VI semiconductor quantum well structures composed of PbSe wells and $Pb_{1-x}Sr_xSe$ barrier materials.

In this study, we use the referenced model from Khodr *et al*. (1998) to study and calculate the effects of the internal quantum efficiency on the threshold current density $J_{th.}$ The internal quantum efficiency is influenced by Auger recombination and may be readily demonstrated by considering the radiative and non radiative life times. Also, quantum the internal quantum efficiency, along with the gain and internal losses, depends on the growth temperature. Hence, these calculations were done at five different temperatures: 300, 250, 200, 150 and 77 K, respectively.

MATERIALS AND METHODS

The system under investigation is PbSe/$Pb_{0.934}$ $Sr_{0.066}$ Se Multiple Quantum Well (MQW) with PbSe as the well material with width of 7 nm and Pb $_{0.934}$ $Sr_{0.066}$ Se as barrier material with thickness of 70 nm, number of wells of 7, index of refraction of the well material is 4.865 and that of the barrier material is 4.38.

Within the framework of Fermi's Golden Rule, the two major components of gain calculations are the electron and whole density of states and the transition matrix element describing the interaction between the conduction and valence band states. The derivation for the analytical gain expression is given by the following expression (Khodr *et al*., 1996, 1998):

$$\gamma(\omega_o) = \frac{\pi e^2 \hbar \rho_{red}}{\varepsilon_o n_{r,w} c m_o^2 w} \frac{\left|M_{QW,n}\right|^2_{avg}}{\hbar\omega_o} [f_c(\omega_o) - f_v(\omega_o)] \sum_{n=1}^{\infty} H(\omega_o - \omega_n) \quad (1)$$

And the component of the carrier recombination is found from the spontaneous emission rate:

$$R_{sp}(\hbar\omega_o) = \frac{e^2 n_{r,w} \hbar\omega_o \rho_{red}}{\eta\pi m_o^2 \varepsilon_o \hbar^2 c^3 w} \left|M_{conv}\right|^2_{avg} f_c(\omega_o) \cdot [1 - f_v(\omega_o)] \cdot \sum_{n=1}^{\infty} H(\omega_o - \omega_n) \quad (2)$$

From this, the current density is calculated by the following equation:

$$J = ew \sum R_{sp}(\hbar\omega_o) \Delta\hbar\omega_o \quad (3)$$

where,

e : The charge of the electron
m_o : The electron free mass

η : The internal quantum efficiency
c : The speed of light
w : The well width
$n_{r,w}$: The index of refraction at the lasing frequency ω_o
ε_o : The permittivity of free space,
$\left|M_{QW,n}\right|^2_{avg}$: The transmission matrix element
ρ_{red} : The reduced density of states,
$f_{c,v}(\omega_o)$: The Fermi-Dirac distribution functions,
$H(x)$: The Heaviside function that is equal to unity when $x>0$ and is zero when $x<0$ and
$\hbar\omega_n$: The energy difference between the bottom of the n-subband in the conduction band and the n-subband in the valence band.

The excitation method that is of importance in this study is injection of carriers into the active region by passing current through the device. An increase in the pumping current leads to an increase in the density of injected carriers in the active region and with it, an increase in the quasi-Fermi levels.

In laser oscillators, the concern is with the modal gain rather with the maximum gain. The modal gain is defined as the gain experienced by the traveling laser mode. It is obtained by multiplying the maximum gain values given by Eq. (1) by the confinement factor. The optical confinement factor depicts the overlap of the optically guided wave with the quantum well. In order for laser oscillation to occur, the modal gain $g_{\mathrm{mod}}(\hbar\omega)$ at the lasing photon energy $\hbar\omega$ must equal the total losses α_{total} given by the following equation:

$$\alpha_{total} = \Gamma_o^{QW}\alpha_{fc} + \alpha_s + \frac{1}{2L}\ln\frac{1}{R_1R_2} \quad (4)$$

where,
Γ_o^{QW} : The confinement factor for the particular structure
α_{fc} : The free carrier absorption
α_s : The scattering loss due to waveguide imperfections

The temperature dependence of α_{total} is contained in the first two terms. The loss due to radiation from the ends of the laser is given by the third term in Eq. 4, where L is the laser cavity length and R_1, R_2 are the end facet reflectivity' s.

The current needed to compensate for the total loss α_{lotal} is called the threshold current (I_{th}) and is calculated by the usual formula:

$$I_{th} = J_{th} \times Area = J_{th} \times L \times width \quad (5)$$

Assuming the cavity width has a constant value of 20 μ m and the mirror reflectivities fixed at $R_1 = 0.4$ and $R_2 = 0.4$, the threshold current density (J_{th}) corresponds to the modal gain value that satisfies the oscillation condition Eq. (4) and can be obtained from the modal gain-current density plots.

The influence of Auger recombination on the quantum efficiency may be readily demonstrated by considering the radiative lifetime τ_r and Auger lifetime τ_a. The radiative recombination rate Rr varies with injected carrier density as:

$$R_r = Bn^2 \quad (5)$$

where,

$$n \cong p$$

The radiative lifetime is given by:

$$\tau_r = n/R_r = 1/Bn \quad (6)$$

where,
B : The radiative constant

The nonradioactive Auger recombination rate R_a varies as:

$$R_a = Cn^3 \quad (7)$$

where,
C: The Auger coefficient. The Auger lifetime becomes:

$$\tau_a = 1/Cn^2 \quad (8)$$

The overall lifetime is:

$$\tau = \tau_a\tau_r/(\tau_a+\tau_r) \quad (9)$$

And the quantum efficiency is:

$$\eta = 1/(1+\tau_r/\tau_a) \quad (10)$$

Substitute for τ_r and τ_a from Eq. (6) and (8):

$$\eta = 1/(1+Cn/B) \quad (11)$$

The temperature dependence of η is contained in B, C and n.

For PbSe, the radiative B coefficient is 10^{-10} cm^3/s and Auger coefficient C is 8×10^{-28} cm^6/s (Hanna *et al*., 2005). Because the temperature dependence of B is believed to be small, B will be taken as constant with temperature. As for Auger coefficient C the value given is approximately constant between 300 and 70K and then drops to a value about 1×10-8 cm^6/s (Hanna *et al*., 2005). The remaining temperature-dependent quantity is the carrier density at threshold n_{th}. The values of nth at the five temperatures of interest in this study are

calculated and accounted for in the software program, hence the theoretical internal quantum efficiency values were obtained using Eq. (11). On the other hand, the experimental values of nth at the five temperatures of interest in this study were obtained from Fig. 1 (Findlay *et al*., 1998), hence the experimental internal quantum efficiency values were obtained using Eq. (11).

The temperature dependence of the gain is first introduced by taking the quantum efficiency $\eta = 1$ at all temperatures. Then we included and calculated the effects of internal losses and quantum efficiency on the behavior of the modal gain, threshold current and threshold current density of the system.

RESULTS AND DISCUSSION

The behavior of the modal gain vs. current density values assuming $\eta = 1$ at five different temperatures: 77, 150, 200, 250 and 300 K, respectively is shown in Fig. 1. The effects of quantum efficiency can be seen in Fig. 2 and as shown in this figure, the current density increases almost 10 times with no effect on the modal gain values. From these figures one notice that the transparency current J_0 (intercept at gain = 0) increases with increasing temperature. Moreover, the slope of the gain versus current density plot decreases with increasing temperature. These two quantities are important in calculating the characteristic temperature T_0 for the system.

The calculated threshold current values are shown in Fig. 3 assuming $\eta = 1$ and Fig. 4 with quantum efficiency values included. Inclusion of the quantum efficiency increases the threshold current value by almost 10 folds. Also, we included the experimental quantum efficiency obtained from Findlay *et al*. (1998). From these figures, one notices that the threshold current curves have a minimum threshold current value at a critical cavity length. The region above the critical thickness value corresponds to the low modal gain regime (or low losses regime). However, the region below the critical cavity length value corresponds to the high modal gain regime (or high losses regime). The threshold current value for the experimental quantum efficiency is much higher than that value for the theoretical quantum efficiency due to leakage current over the barrier.

The threshold current density curves for $\eta = 1$ and $\eta \neq 1$ are shown in Fig. 5 and 6, respectively. As seen in these figures, these values increase with temperature increase at any fixed cavity length. Also, it can be noticed that the threshold current density values drops fast at small cavities and remains constant after some critical cavity length around 100 μm. The effects of quantum efficiency are clear in that it increases the threshold current density values. We included the experimental quantum efficiency values to calculate the current density values at 300K and the results are

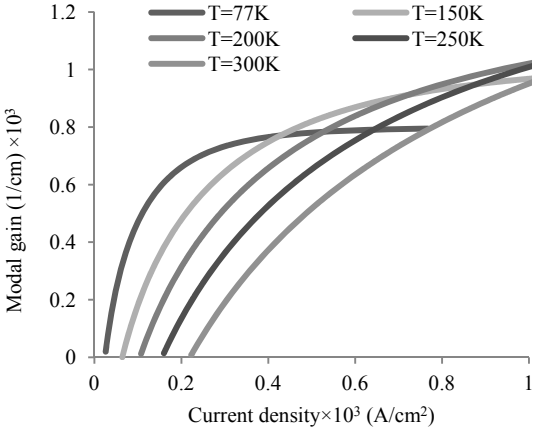

Fig. 1: The modal gainassuming unity quantum efficiency

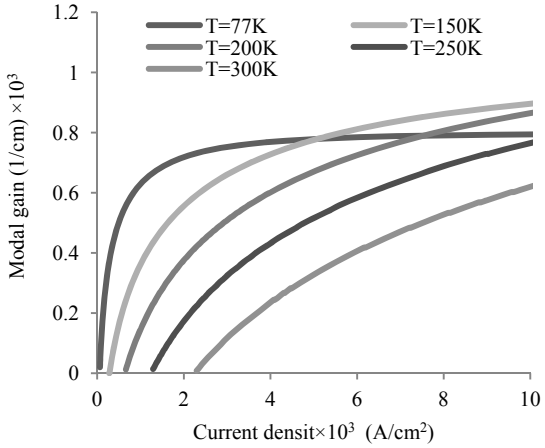

Fig. 2: The modal gain values including the effect of quantum efficiency

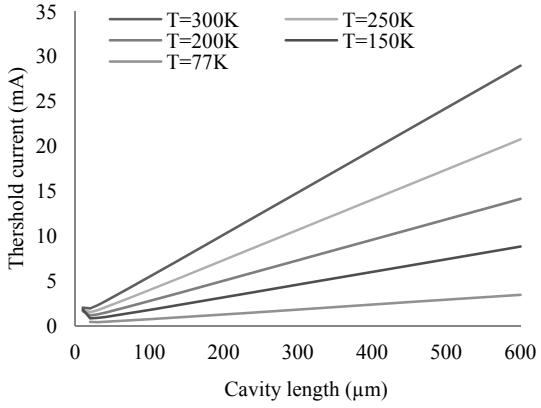

Fig. 3: Threshold current assuming unity quantum efficiency

shown in Fig. 6. From this figure one notices that the threshold current density values using the experimental quantum efficiency values are higher than the theoretically assumed ones. Similar to threshold current, this indicates that there is an addition factor affecting the current density value and it could be due

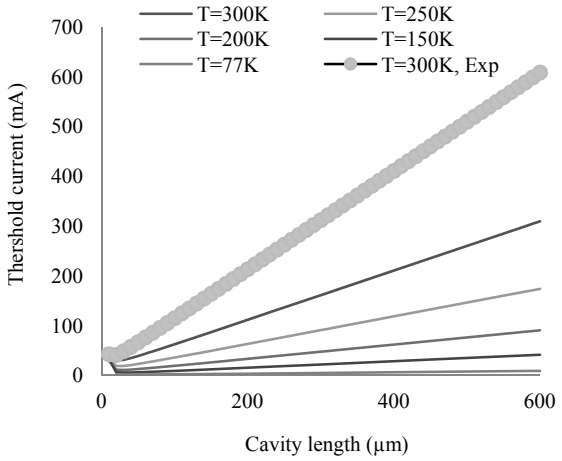

Fig. 4: Threshold current values including the theoretical and experimental quantum efficiency

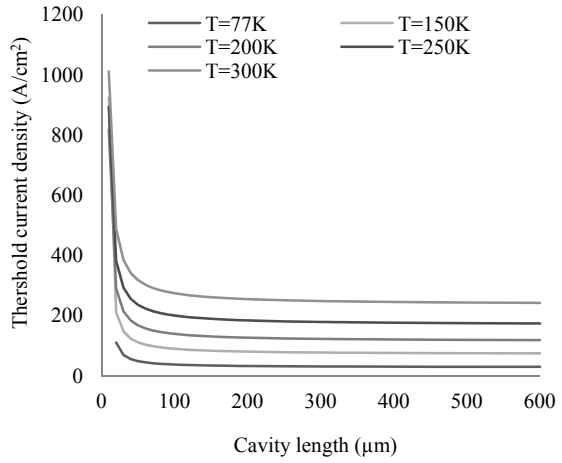

Fig. 5: Threshold current density assuming unity quantum efficiency

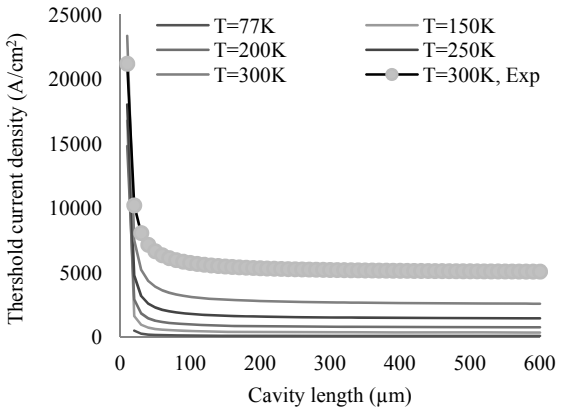

Fig. 6: Threshold current density including the theoretical and experimental quantum efficiency

to leakage current over the barrier. Leakage current calculations will be addressed in future publications.

CONCLUSION

The effects of temperature and quantum efficiency on the threshold current density and threshold current values of PbSe/$Pb_{0.934}$ $Sr_{0.066}$ Se multiple Quantum well Structure were calculated. Inclusion of quantum efficiency increased the threshold current values by almost 10 times. Also, it was noticed that the threshold current density values dropped fast at small cavities and remained constant after some critical cavity length around 100 μm. When experimental quantum efficiency values were used, the threshold current values were higher than those found using the theoretical quantum efficiency values. This indicates that there is an additional factor affecting the current density values and it could be due to leakage current over the barrier, which we will account for in future work.

REFERENCES

Findlay, P.C., C.R. Pidgeon, R. Kotitschke, A. Hollingworth, B.N. Murdin, C.J. Langerak, A.F. Van der Meer, C.M. Ciesla, J. Oswald, A. Homer, G. Springholz and G. Bauer, 1998. Auger recombination dynamics of lead salts under picosecond free-electron-laser excitation. Phys. Rev. B, 58: 12908-12915. http://journals.aps.org/prb/abstract/10.1103/PhysRevB.58.12908.

Hanna, M.C., R.J. Ellingson, M. Beard, P. Yu, O.I. Micic and A.J. Nozik, 2005. Quantum dot solar cells: High efficiency through multiple exciton generation. Proceeding of the DOE Solar Energy Technologies Program Review Meeting DOE/GO-102005-2067. http://en.coe.pku.edu.cn/Faculty-A-Z/120. htm.

Khodr, M.F., B.A. Mason and P.J. McCann, 1996. Effects of band Non-parabolicity on the gain and current density in EuSe/$PbSe_{0.78}Te_{0.22}$/EuSe IV-VI semiconductor quantum well lasers. IEEE J. Quantum Elect., 32(2): 236-247. http://ieeexplore.ieee.org/xpl/articleDetails.jsp?reload=true&arnumber=481871.

Khodr, M.F., B.A. Mason and P.J. McCann, 1998. Optimizing and engineering EuSe/PbSe0.78Te 0.22/EuSe multiple quantum well laser structures. IEEE J. Quantum Elect., 34(9): 1604-1611. http://ieeexplore.ieee.org/xpl/login.jsp?tp=&arnumber=709577&url=http%3A%2F%2Fieeexplore.ieee.org%2Fxpls%2Fabs_all.jsp%3Farnumber%3D709577.

Kim, C.S., C.L. Canedy, E.H. Aifer, M. Kim, W.W. Bewley *et al*., 2007. Molecular beam epitaxy growth of antimonide type-II "W" high-power interband cascade lasers and long-wavelength infrared photodiodes. J. Vac. Sci. Technol. B, 25: 991-994. http://scitation.aip.org/content/avs/journal/jvstb/25/3/10.1116/1.2484728.

Lehtinen, J. and T. Kuusela, 2014. Broadly tunable quantum cascade laser in cantilever-enhanced photoacoustic infrared spectroscopy of solids. Appl. Phys. B, 115(3): 413-418. http://link.springer.com/article/10.1007%2Fs00340-013-5617-9.

Razeghi, M., N. Bandyopadhyay, Y. Bai, Q. Lu and S. Slivken, 2013. Recent advances in mid infrared (3-5μm) quantum cascade lasers. Opt. Mater. Express, 3(11): 1872-1884. https://www.osapublishing.org/ome/abstract.cfm?uri=ome-3-11-1872.

Yang, R., C. Hill and B. Yang, 2005. High-temperature and low-threshold mid-infrared interband casade lasers. Appl. Phys. Lett., 87: 151109. http://scitation.aip.org/content/aip/journal/apl/87/15/10.1063/1.2103387.